EEET ECOLOGICAL ENGINEERING & ENVIRONMENTAL TECHNOLOGY

Ecological Engineering & Environmental Technology, 2026, 27(10), 274–290
https://doi.org/10.12912/27197050/231654
ISSN 2719–7050, License CC-BY 4.0

Received: 2026.07.27
Accepted: 2026.08.31
Published: 2026.09.10

Hydrodynamic effects on bulk-suspension microbial abundance and a preliminary conceptual safe operating window for bioelectrochemical systems

Fitria Nur Laily[1*], Juwari[1,2], Sri Rachmania Juliastuti[2], Dhia Fairuz Shabrina[3,4], Adlina Taufik Syamlan[3,5]

[1] Process Safety Engineering, Department of Mechanical Engineering, Institut Teknologi Sepuluh Nopember, Jl. Raya ITS, Keputih, Surabaya 60111, Indonesia
[2] Department of Chemical Engineering, Institut Teknologi Sepuluh Nopember, Jl. Raya ITS, Keputih, Surabaya 60111, Indonesia
[3] Department of Mechanical Engineering, Institut Teknologi Sepuluh Nopember, Jl. Raya ITS, Keputih, Surabaya 60111, Indonesia
[4] Department of Mechanical Engineering, The University of Melbourne, Grattan Street, Parkville Victoria 3010, Australia
[5] Department of Mechanical Engineering, KU Leuven, De Nayer Campus, 2860 Sint-Katelijne-Waver, Belgium
* Corresponding author's e-mail: fitrianurlaily@its.ac.id

ABSTRACT

Hydrodynamic conditions can influence mass transfer, suspended-cell distributions, and electrode-associated biofilms in bioelectrochemical systems. This study evaluated mechanical agitation in a batch single-chamber microbial fuel cell (MFC) and developed a preliminary conceptual Safe Hydrodynamic Operating Window (SHOW) framework. The surviving archive contains one bulk-suspension microbial count for each of six agitation conditions (0, 50, 100, 150, 200, and 250 rpm) on days 0, 5, 10, 15, and 20, yielding 30 longitudinal observations. Counts were obtained by direct microscopic enumeration after a 1-g bulk-reactor sample was diluted in demineralized water to 10^{-5}; five counting-chamber areas were read and the mean was converted to cells mL^{-1}. The mean across the five sampled days decreased descriptively from 6.644×10^6 cells mL^{-1} at 0 rpm to 3.32×10^5 cells mL^{-1} at 250 rpm, a 95.0% difference. Because these values are repeated time points and the archive does not document independent reactor replication, no independent-groups inferential test or statistically validated rpm threshold is claimed. The 50–150 rpm interval is retained only as a hypothesis-generating candidate region for future validation. The measured fraction was bulk reactor suspension, not scraped or eluted electrode biomass; therefore, direct biofilm retention and detachment were not measured. Validation of SHOW requires independent reactors together with biofilm, hydrodynamic, electrochemical, treatment-performance, energy, and reliability measurements.

Keywords: bioelectrochemical system, bulk suspension, direct microscopic counting, hydrodynamics, microbial fuel cell, inherently safer design, conceptual operating window, safe hydrodynamic operating window.

INTRODUCTION

Bioelectrochemical systems are technologies that utilize microbial activity to catalyze electrochemical reactions and convert chemical energy stored in organic matter into electrical energy or other value-added products. One of the most extensively developed configurations is the microbial fuel cell (MFC), which employs electroactive microorganisms to oxidize organic substrates and transfer the resulting electrons to the anode. The electrons subsequently flow through an external circuit toward the cathode, thereby generating an electrical current. Through this

mechanism, MFCs offer the potential to integrate wastewater treatment, resource recovery, and energy generation within a relatively simple system (Logan et al., 2006; Santoro et al., 2017).

A wide variety of substrates have been applied in MFCs, ranging from simple organic compounds to domestic, industrial, agricultural, and food wastes. This substrate flexibility makes MFCs attractive as an alternative waste-treatment technology that can simultaneously generate energy. Nevertheless, the electrical output of MFCs generally remains insufficient for large-scale commercial applications. System performance is also influenced by reactor configuration, substrate properties, electrode surface area, electrode spacing, internal resistance, electrolyte conductivity, microbial communities, and operating conditions (Pant et al., 2010; Slate et al., 2019). Therefore, MFC development requires not only improvements in electrochemical activity but also effective control of process conditions to maintain biological and electrochemical stability during operation.

The scale-up of MFCs continues to face challenges in maintaining uniform distributions of substrates, flow, electrical potential, and microbial activity. The use of stacked MFC configurations can increase the total voltage and current; however, it may also create performance imbalances among individual units and increase system complexity (Aelterman et al., 2006). Increasing reactor dimensions may also extend ion-transport distances, increase internal resistance, and create nonuniform flow zones. Consequently, operating conditions that provide satisfactory performance in laboratory-scale reactors may not produce the same response at larger scales. Practical MFC implementation therefore requires an integrated approach that considers reactor design, flow distribution, electrode area, additional energy consumption, and long-term operational stability (Corona-Martínez et al., 2025; Fathima et al., 2024).

One of the principal biological components determining MFC performance is the electroactive biofilm formed on the anode surface. Electroactive microorganisms oxidize organic compounds and transfer electrons to the electrode through direct contact, redox mediators, outer-membrane cytochromes, or conductive structures such as microbial nanowires. Biofilm formation on the electrode increases contact between microorganisms and the conductive surface, thereby supporting sustained extracellular electron transfer. Studies of Geobacter sulfurreducens, for example, have demonstrated that microbial colonization of electrode surfaces is associated with electrical-current generation, while biofilm and conductive-structure production can enhance electron transfer through the microbial community (Bond & Lovley, 2003; Reguera et al., 2006). MFC biofilm models have also demonstrated that electrical output results from interactions among microbial kinetics, biofilm conductivity, mass transfer, and potential distribution within the biofilm layer (Marcus et al., 2007; Picioreanu et al., 2007).

A biofilm is a community of microorganisms attached to a surface and organized within a matrix of extracellular polymeric substances (EPS). This matrix may comprise polysaccharides, proteins, lipids, extracellular nucleic acids, water, and various other components that maintain biofilm structure. EPS strengthens cell–surface adhesion, enhances cell–cell cohesion, retains water and nutrients, and protects microorganisms from changes in environmental conditions. Biofilm development generally proceeds through cell transport toward the surface, reversible adhesion, irreversible attachment, microcolony formation, maturation, and partial biomass release into the surrounding environment (Flemming et al., 2016, 2023). Successful initial adhesion is influenced by cell properties, surface charge, hydrophobicity, electrode roughness, medium composition, and physicochemical interactions between microbial cells and the surface (Petrova and Sauer, 2012).

Although biofilm formation is essential for MFC function, a greater amount of biomass does not necessarily indicate better bioelectrochemical performance. An excessively thick biofilm may develop regions with limited access to substrates, ions, or electron acceptors. Cells located farther from the electrode surface may also experience longer electron-transfer pathways and lower electrochemical activity. In porous electrodes, biofilm growth and its contribution to current generation may decrease with increasing pore depth because of mass-transfer limitations (Yang et al., 2023). Biofilm heterogeneity can also produce nonuniform distributions of substrates and metabolic products, causing a portion of the biomass to function as a transport barrier and an additional source of resistance rather than as an effective biocatalyst (Chen et al., 2024). Biofilm management should therefore aim to maintain active and stable biomass that remains effectively connected to the electrode rather than merely maximizing the total microbial population.

Conversely, insufficient biomass retention may reduce the proportion of the electrode surface covered by electroactive microorganisms. Excessive biomass loss may decrease substrate-oxidation capacity, reduce current generation, and prolong recovery following an operational disturbance because the electrode surface must be recolonized. Research on biofilm revitalization has demonstrated that controlled hydrodynamic shear can remove inactive cells and support stable power generation. However, excessive shear forces may detach active biomass and impair bioelectrochemical function (Islam et al., 2019). The desired biofilm condition therefore lies within a balance among microbial growth, activity, adhesion, and detachment.

One of the primary factors governing this balance is the hydrodynamic condition surrounding the electrode surface. Hydrodynamics control the transport of planktonic cells toward the surface, the distribution of substrates and ions, the removal of metabolic products, the thickness of the mass-transfer boundary layer, and the mechanical forces acting on the biofilm. Under very low-flow conditions, mass transfer becomes increasingly dependent on diffusion, potentially resulting in concentration gradients and stagnant zones. Increasing flow or agitation may improve external mass transfer and enhance contact among microbial cells, substrates, and electrodes. However, increasing hydrodynamic intensity also increases shear stress, which may alter biofilm structure, density, thickness, and adhesion strength (Liu and Tay, 2002; Stoodley et al., 1999).

The influence of shear stress on biofilm development is not uniform. Moderate shear may produce a thinner, denser, and stronger biofilm by removing weakly attached biomass. Such conditions may also improve substrate supply to metabolically active regions of the biofilm. Conversely, when the applied mechanical force exceeds the adhesive strength of microbial cells or the cohesive strength of the EPS matrix, the biofilm may undergo erosion, sloughing, and detachment. Studies of electroactive biofilms have shown that shear stress affects growth rate, thickness, surface coverage, the proportion of active microorganisms, microbial-community composition, and MFC electrochemical performance (Godain et al., 2024). The relationship between hydrodynamic intensity and biofilm performance is therefore likely to be nonlinear because both insufficient mixing and excessive shear may produce undesirable biological conditions.

In fluid systems more generally, hydrodynamic characteristics are governed not only by flow velocity but also by equipment geometry and internal configuration. Aopik and Dwiyantoro (2023) demonstrated that modifications to reducer geometry and adjuster-opening conditions influenced pressure drop, backflow, and vortex formation in a piping system. Sasongko and Rahman (2023) similarly showed that damper-plate configuration, nozzle geometry, and flow rate produced different vortex characteristics and flow kinetic energies. Although these studies did not investigate biofilms, their findings support the fundamental fluid-mechanical principle that a single velocity or flow-rate value cannot be interpreted independently of system geometry. In MFCs, electrode positioning, reactor geometry, impeller configuration, liquid volume, and spatial distribution may similarly determine the local shear and mass-transfer conditions experienced by the biofilm.

Interactions among flow patterns, substrate consumption, and current generation have also been demonstrated through MFC modeling. Non-uniform velocity distributions may create spatial differences in substrate concentration and electrochemical activity within a reactor (Day et al., 2022). During scale-up, interactions among internal structures may become increasingly complex. Wulaningtyas and Yuwono (2025), for example, demonstrated that rotor spacing in a hydrokinetic-turbine system affected wake interactions and the performance of individual turbines. Although this system differs from an MFC, the findings demonstrate that changes in system dimensions and component arrangements may create flow interactions that are not observed in isolated components. This supports the need to reassess hydrodynamic conditions whenever the configuration or scale of an MFC is modified.

The importance of controlling operating parameters has also been demonstrated in other biomass-conversion systems. Nugroho et al. (2026) showed that temperature, pressure, biomass-to-water ratio, residence time, and particle-flow dynamics jointly influenced biomass conversion in a hydrothermal reactor. These findings indicate that the performance of a biomass-based process is determined not only by feedstock characteristics but also by the ability of the system to maintain an appropriate combination of operating conditions. A similar principle applies to MFCs because hydrodynamic conditions interact with substrate

composition, microbial-community activity, electrode condition, and biofilm-development stage. Operating-condition selection should therefore be based on a parameter range that provides an acceptable combined response rather than on a single optimum value.

Biofilm imbalance resulting from inappropriate hydrodynamic conditions may develop into operational problems. Insufficient mixing may increase the likelihood of stagnant zones, non-uniform substrate distribution, excessive biomass accumulation, and increased electrode-cleaning requirements. Conversely, excessive agitation may cause biomass loss, decrease biocatalyst coverage, and extend the recovery period following disturbances. Unwanted microbial colonization of the cathode may also cover active sites and restrict oxygen transfer, thereby reducing cell potential and power output during long-term operation (Barakat et al., 2025). These problems demonstrate that biofilm control is related not only to biological performance but also to reliability, maintenance, energy consumption, and operational continuity.

From a process-safety perspective, hydrodynamic conditions can be treated as operating variables that should be maintained within an acceptable range. This approach is consistent with inherently safer design (ISD), which prioritizes hazard reduction through changes in materials, technology, inventories, design, or operating conditions before relying on additional protective layers. The four principal ISD strategies are minimize, substitute, moderate, and simplify. In the context of biofilm control, the most relevant strategies are moderation, which involves avoiding excessively severe operating conditions, and simplification, which involves establishing operating guidance and deviation-response procedures that are clear and practical (Center for Chemical Process Safety, 2019; Hendershot, 2012).

The application of ISD principles does not imply that agitation control automatically renders an MFC risk-free. Agitators, motors, sensors, alarms, and control systems remain active protective measures that may themselves fail. Nevertheless, selecting hydrodynamic conditions that do not promote either excessive biomass accumulation or excessive biomass loss may reduce the system's dependence on cleaning, reinoculation, and other corrective interventions. ISD principles should therefore be integrated with hazard analysis, operating procedures, equipment integrity, management of change, training, inspection, and maintenance (Amyotte and Khan, 2021; Rayner Brown et al., 2021).

Structured risk management generally requires hazard identification, risk assessment, prioritization, and the development of appropriate control measures. Akbar et al. (2025) applied the HIRARC approach to connect facility conditions, potential hazards, risk levels, and control measures in pumphouse facilities. Although that study focused on occupational health and safety rather than MFC operation, its approach supports the need to translate technical-analysis results into clearly defined indicators, limits, and control actions. In bioelectrochemical systems, deviations caused by insufficient mixing or excessive agitation should similarly be connected to biological, electrochemical, operational, and maintenance indicators.

Previous studies of biofilm hydrodynamics have primarily focused on the effects of flow velocity or shear stress on microbial adhesion, morphology, thickness, community composition, mass transfer, and electrochemical performance. These investigations provide an important basis for understanding biofilm formation and function. However, limited attention has been given to translating biological and hydrodynamic observations into structured operating guidance from a process-safety perspective. In particular, operating-window frameworks that simultaneously consider two opposing conditions—excessive biomass accumulation under insufficient hydrodynamic intensity and biocatalyst loss under excessive hydrodynamic intensity remain underdeveloped.

The identification of a single agitation speed as an optimum operating condition may also imply an inappropriate level of certainty for a biological system. Biofilm responses to agitation may change with biofilm age, substrate composition, microbial concentration, fluid properties, microbial-community activity, electrode condition, reactor geometry, and operating phase. Furthermore, rotational speed is specific to the equipment configuration and does not directly represent the shear stress experienced by the biofilm. A more transferable operating window should ultimately incorporate variables such as shear rate, shear stress, Reynolds number, power input per unit volume, mixing time, and superficial velocity, together with biological, electrochemical, treatment-performance, and energy-consumption responses.

Based on this research gap, the present study aimed to describe the influence of mechanical

agitation on bulk-suspension microbial abundance in a single-chamber MFC. Six nominal agitation conditions 0, 50, 100, 150, 200, and 250 rpm, were followed on days 0, 5, 10, 15, and 20. The measured response was total cell concentration in a bulk reactor sample; electrode-associated biomass, biofilm thickness, attachment, and detachment were not measured directly. The observed time courses were interpreted descriptively alongside literature-supported biofilm and mass-transfer mechanisms.

The principal contribution of this study is not a new agitation methodology; the archived 0–250 rpm time course and direct microscopic counts are methodologically straightforward. The novelty claimed here lies in translating a limited biological observation into a process-safety-oriented, preliminary conceptual SHOW framework while explicitly separating measured evidence from mechanism-based hypotheses. No numerical safety boundary, universally optimal rpm, causal biofilm mechanism, or validated safety margin is claimed.

MATERIALS AND METHODS

Experimental design

The study archive contains six nominal agitation conditions (0, 50, 100, 150, 200, and 250 rpm) and one microbial-count time series for each condition. Samples were recorded on days 0, 5, 10, 15, and 20, giving 30 observations. The five values per agitation condition are longitudinal time points, not five independent biological or reactor replicates. No reactor-level replicate identifier is preserved in the archive. Agitation speed was the controlled variable and bulk-suspension total cell concentration was the measured response; the dataset was therefore summarized descriptively.

MFC construction and operation

A single-chamber MFC with a nominal working volume of 1 L was filled with 500 mL of hydrolyzed food-waste substrate and 500 mL of Sidoarjo mud. The anode and cathode were prepared from carbon cloth (Twill A-2205, Shanghai Passion Composites Co., Ltd., China), approximately 5 × 2 × 2 mm, and connected with copper wire. Before use, the carbon cloth was sequentially immersed in 1 M hydrochloric acid for 24 h and 1 M sodium hydroxide for 24 h, followed by rinsing with distilled water. The construction of the MFC system is shown in Figure 1.

The anode was positioned approximately 3 cm above the reactor bottom, while the cathode was placed near the liquid surface. Both electrodes were connected through a 1000-Ω external resistance. Each reactor received 20 mL of Shewanella oneidensis MR-1 culture after 10 h of cultivation and 1 mL of cobalt micronutrient solution. The MFCs were operated in batch mode under the designated nominal rotational setpoints. The surviving records do not retain the agitator or impeller model, dimensions, position, or calibration; consequently, rpm is treated as equipment-specific and is not converted to shear stress or power input.

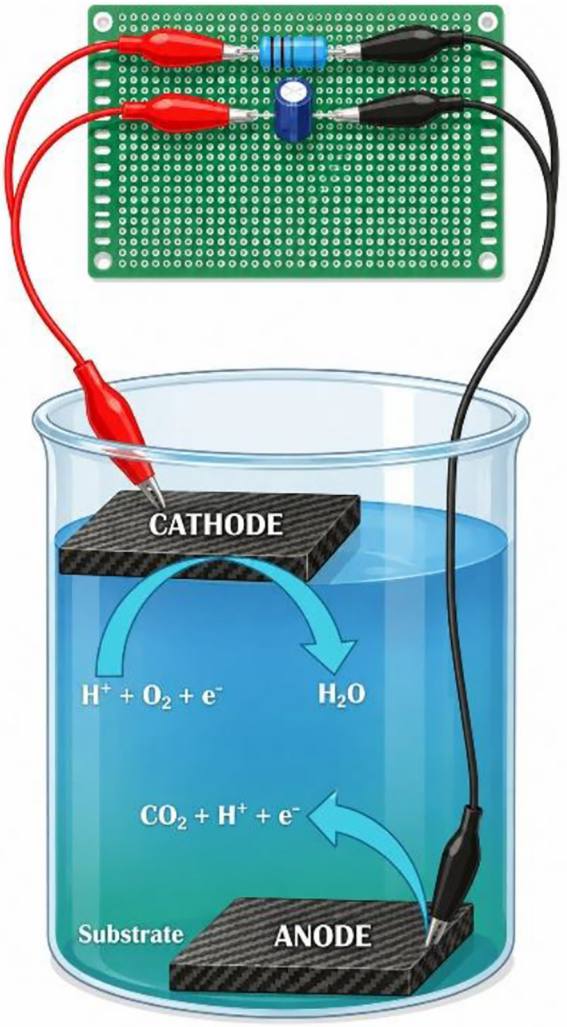

Figure 1. Schematic representation of the single-chamber microbial fuel cell and the nominal mechanical agitation conditions

Microbial culture and substrate preparation

Shewanella oneidensis MR-1 ATCC 700550 was activated in nutrient broth at 30 °C; a growth curve was previously used to identify the log-phase cultivation period, and the culture used for MFC inoculation was harvested after 10 h. The hydrolytic cultures were Aspergillus oryzae RIB40 (ATCC 42149), Aspergillus aculeatus Iizuka 36411, and Candida rugosa NCPF 8452, activated in yeast extract-peptone-dextrose medium at 30 °C. Food waste was homogenized and mixed with distilled water at a volume ratio of 333:167 mL, after which the three hydrolytic cultures were added under log-phase conditions and hydrolysis proceeded for 24 h. Sidoarjo mud, used as an additional source of indigenous microorganisms, was collected from approximately 30–45 cm depth in Renokenongo Village, Porong, East Java, Indonesia (approximately 7°31′45.6″ S, 112°42′43.6″ E).

Microbial enumeration and data analysis

Samples represented the bulk reactor matrix (the liquid–slurry mixture of hydrolyzed food-waste substrate and Sidoarjo mud), not an electrode scraping or eluted electrode-associated fraction. A 1.00-g aliquot of reactor contents was collected on days 0, 5, 10, 15, and 20. The sample was diluted with demineralized water through five successive tenfold dilutions to an overall dilution factor of 10^{-5}, placed in a counting chamber, and examined by direct microscopy at 40× magnification. Five chamber areas recorded as A–E were counted, and their arithmetic mean was used in the archived calculation: cell concentration (cells mL^{-1}) = mean chamber-area count × 10^4 × 10^5. This was a direct total-cell count; viability was not assessed. No culture medium, plated volume, spread/pour-plating technique, incubation temperature or duration, technical plate replicate, colony-forming-unit calculation, or colony-countability range applies. The counting-chamber manufacturer/model, loaded volume, exact serial-transfer volumes, boundary-counting convention, and storage interval were not retained; the archived method describes dilution followed by direct counting (Laily et al., 2023). The underlying A–E chamber readings for the present 30 reported values were not preserved.

All 30 archived observations are reported in Table 1 and Supplementary Data S1. For each agitation condition, the mean, standard deviation, median, minimum, and maximum across the five sampled days were calculated only as descriptive summaries of the observed time course. Welch ANOVA, Games–Howell comparisons, and other independent-groups tests were not used because the five values are repeated time points and independent reactor replication is not documented. The data therefore support descriptive and hypothesis-generating interpretation only.

RESULT AND DISCUSSION

Observed bulk-suspension microbial response and mechanistic context

Hydrodynamic conditions are among the principal factors governing microbial transport and biofilm development in bioelectrochemical systems because they can influence cell transport, nutrient distribution, boundary-layer thickness, extracellular polymeric substances, and mechanical forces at the electrode (Godain et al., 2024; Logan et al., 2019). In the present experiment, however, only bulk-suspension total cell concentration was measured. The following biofilm interpretation is therefore literature-supported mechanistic context rather than a direct observation of electrode-associated biomass.

Biofilm formation begins with the transport of planktonic cells toward a solid surface through diffusion, sedimentation, and convection, as summarized in Figure 2. After reaching a surface, cells may undergo reversible and then irreversible attachment, followed by extracellular-polymeric-substance production and community development (Flemming et al., 2023; Petrova and Sauer, 2012). A bulk-suspension count cannot determine how many cells reached or remained on the electrode and cannot distinguish growth, attachment, erosion, detachment, or loss of viability.

Hydrodynamics affect this process through two competing mechanisms. On the one hand, enhanced mixing improves mass transfer and increases the transport of microbial cells, nutrients, ions, and metabolites to and from the biofilm surface. A thinner mass-transfer boundary layer can accelerate substrate delivery and metabolic-product removal, thereby supporting microbial activity (Chen et al., 2024; Logan et al., 2019). On the other hand, increasing fluid velocity also increases hydrodynamic shear stress. When the imposed stress exceeds the strength of initial adhesion or

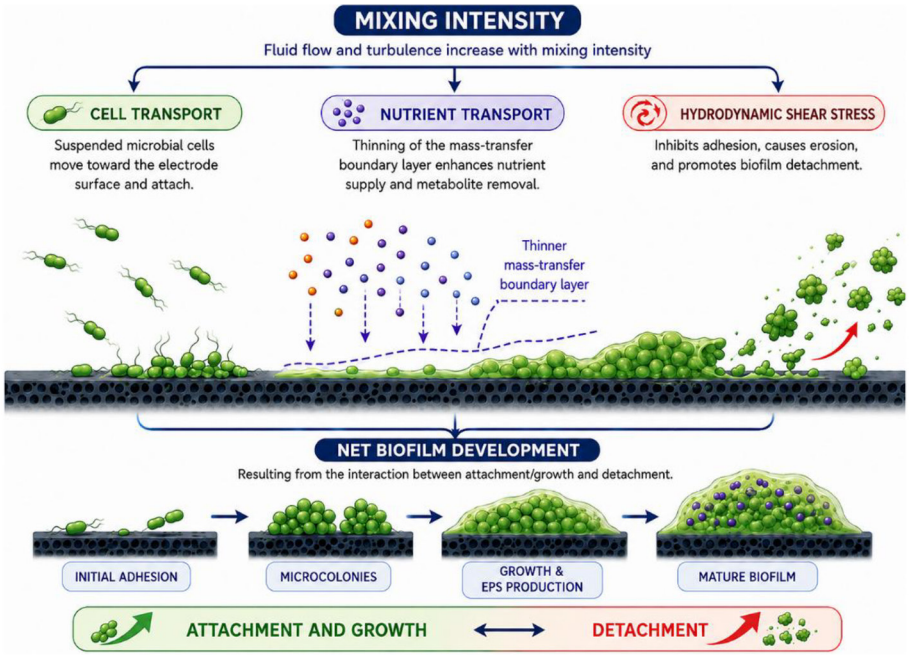

Figure 2. Proposed hydrodynamic mechanisms governing biofilm development in microbial fuel cells

the cohesive strength of the EPS matrix, the biofilm may undergo erosion, sloughing, or detachment, thereby reducing the amount of biomass retained on the electrode (Godain et al., 2024; Islam et al., 2019).

Shear stress is therefore not uniformly detrimental. At moderate levels, it may remove weakly attached or inactive biomass and promote a thinner, denser, and more homogeneous electroactive biofilm. Conversely, excessive hydrodynamic intensity can cause the detachment rate to exceed the combined rates of attachment and growth, thereby limiting biofilm development (Godain et al., 2024; Islam et al., 2019). The relationship between hydrodynamics and biofilm formation is consequently nonlinear: both inadequate mixing and excessive agitation can compromise the functional performance of a bioelectrochemical system.

The archived observations show different bulk-suspension microbial-count trajectories across the six nominal agitation conditions. Counts at 0–150 rpm generally increased through day 20, whereas the 200- and 250-rpm series peaked on day 10 and subsequently declined. At day 20, the recorded counts were 9.40×10^6, 6.70×10^6, 6.60×10^6, 6.40×10^6, 1.00×10^6, and 2.00×10^5 cells mL^{-1} at 0, 50, 100, 150, 200, and 250 rpm, respectively

The trajectories are consistent with an agitation-associated difference in bulk-phase cell abundance, but they do not identify its cause. Possible explanations include differences in growth, sedimentation, attachment, shear-related loss, sampling heterogeneity, or combinations of these processes. Because no electrode-associated biomass, cell viability, or local hydrodynamic stress was measured, detachment and biofilm retention remain hypotheses rather than measured outcomes.

Descriptive interpretation of the archived time course

The archived table comprises one observation for each agitation condition at each of five sampling days. This structure is longitudinal and contains no documented independent reactor replication. Treating the five days as five independent replicates would underestimate dependence and create pseudoreplication. Accordingly, interpretation is restricted to the observed trajectories and descriptive summaries.

Across days 0–20, the descriptive mean counts were 6.644×10^6, 3.044×10^6, 2.594×10^6, 2.254×10^6, 1.028×10^6, and 3.32×10^5 cells mL^{-1} at 0, 50, 100, 150, 200, and 250 rpm, respectively. The corresponding medians were 8.22×10^6, 2.70×10^6, 1.90×10^6, 1.60×10^6, 1.00×10^6, and 2.00×10^5 cells mL^{-1}. The mean at 250 rpm was 95.0% lower than the mean at 0 rpm. These summaries describe five temporal observations and are not estimates from independent replicate reactors.

Table 1. Archived longitudinal bulk-suspension microbial counts (cells mL^{-1})

Sampling day	0 rpm	50 rpm	100 rpm	150 rpm	200 rpm	250 rpm
0	1.40×10^6	4.30×10^6	5.60×10^6	3.80×10^6	1.80×10^6	3.00×10^6
5	5.40×10^6	9.90×10^6	7.10×10^6	5.90×10^6	2.60×10^6	1.90×10^6
10	8.22×10^6	2.70×10^6	1.90×10^6	1.60×10^6	1.90×10^6	6.70×10^6
15	8.80×10^6	4.40×10^6	3.20×10^6	2.30×10^6	1.80×10^6	5.70×10^6
20	9.40×10^6	6.70×10^6	6.60×10^6	6.40×10^6	1.00×10^6	2.00×10^6

The complete 30-value matrix in Table 1 shows that temporal behavior differed most clearly above 150 rpm: the 200 and 250 rpm counts increased initially and declined after day 10, whereas the 0–150 rpm series continued to increase through day 20. Because each cell in the design contains one archived observation, the apparent separation should be treated as a descriptive pattern requiring confirmation with independently replicated reactors.

Figure 3 presents the 30 archived observations as time courses rather than as independent-group boxplots. A logarithmic ordinate is used to display the full range of counts. Connecting lines are visual guides and do not imply a fitted kinetic model.

Evidence boundary. Independent-groups inferential tests were removed because the five values per rpm are repeated sampling days, not five documented independent reactor replicates. Therefore, p-values from one-way ANOVA, Welch ANOVA, Tukey, or Games–Howell procedures would not provide a valid test of independent treatment replication for this archive.

The descriptive means decline with increasing nominal rpm, and the day-20 observations show the same broad ordering. Nevertheless, this single archived time series per condition cannot quantify between-reactor uncertainty, establish a causal agitation effect, locate a threshold, or validate a safe operating region.

Biologically, the descriptive differences may reflect changes in the bulk microbial population and/or redistribution between suspended and attached fractions. The present measurements cannot isolate those alternatives. Thus, 0 rpm cannot be designated as the best condition solely because it had the highest bulk count, and the low count at 250 rpm cannot be classified as biofilm failure without direct measurements of electrode-associated biomass, viability, mass transfer, and electrochemical performance.

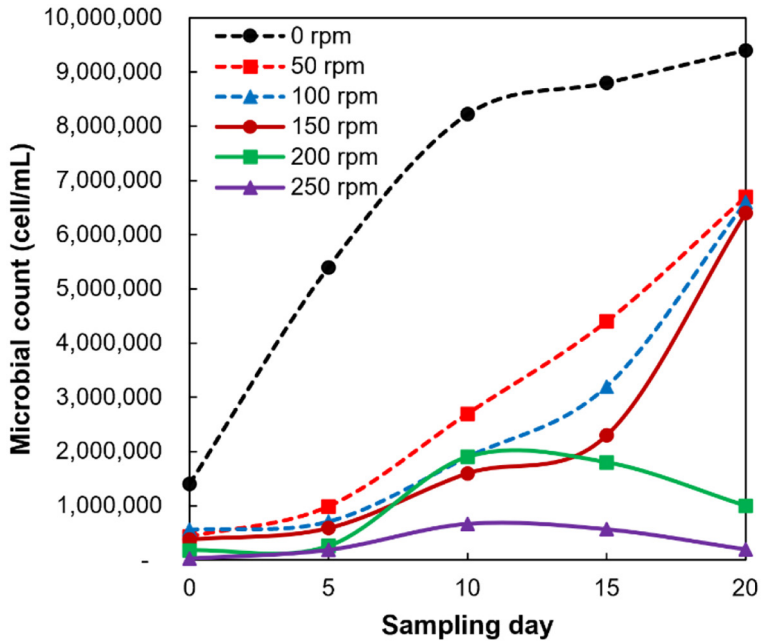

Figure 3. Archived bulk-suspension microbial counts by sampling day and nominal agitation speed

Operational implications for bioelectrochemical systems

The performance of a bioelectrochemical system depends not only on the ability of microorganisms to form a biofilm but also on the ability of the system to maintain that biocatalytic function during operation. In an MFC, electroactive microorganisms oxidize organic substrates and transfer electrons to the electrode. Changes in biofilm condition may therefore affect electrode utilization, extracellular electron transfer, internal resistance, electrical-output stability, and substrate-removal performance. A biofilm with a high cell count does not necessarily provide superior performance if a substantial fraction of the biomass is inactive or poorly connected to the electrode and substrate supply (Logan et al., 2019).

The present study quantified bulk-suspension total cell counts but did not measure electrode-associated biomass, voltage, current density, power density, internal resistance, Coulombic efficiency, chemical oxygen demand removal, biofilm thickness, extracellular polymeric substances, or cell viability at each agitation speed. Consequently, the operational implications discussed here are mechanistic interpretations supported by the literature rather than direct measurements of biofilm or electrochemical performance.

The higher bulk-suspension count observed at 0 rpm indicates greater measured cell abundance in the sampled reactor matrix, not stronger electrode-biofilm retention. Bulk and attached fractions may respond differently, and a high bulk count cannot be equated with maximum electrochemical activity. During prolonged operation, excessive attached biomass could still produce transport limitations or inactive regions, but that possibility was not measured in the present experiment (Islam et al., 2019).

Excessive accumulation may also create electrochemically inactive regions. Cells located close to the electrode generally have better access to direct or mediated electron-transfer pathways, whereas cells located farther from the electrode depend on longer substrate-diffusion and electron-transfer paths. If biomass accumulation is not accompanied by a corresponding increase in accessible electrode area, part of the biofilm may become a transport and resistance burden rather than a functional biocatalyst.

Conversely, the lower bulk-suspension counts observed at 200 and 250 rpm identify a condition that warrants further investigation, but they do not prove insufficient electrode coverage or shear-induced detachment. The decline could reflect lower growth, redistribution to attached biomass, loss from the reactor, reduced viability, or sampling variability. Direct electrode-biomass and electrochemical measurements are required before a low-retention mechanism or operational failure can be assigned.

Total biomass is also an incomplete measure of electrode utilization. Yang et al. (2023) showed that restricted mass transfer within anode pore channels affects biofilm thickness, metabolic activity, community composition, and power generation. In narrow or deep pores, colonization by electroactive microorganisms and current contribution decline because substrate access becomes limited. Thus, a high overall microbial count does not necessarily imply a proportionally larger electrochemically active electrode area.

Biofilm heterogeneity can further create spatial differences in electrode activity. Regions with adequate substrate and ion supply may remain active, whereas transport-limited regions may contain biomass with low metabolic or electrochemical activity. Chen et al. (2024) emphasized that heterogeneous biofilm structures create nonuniform transport pathways for substrates and products, making mass-transfer efficiency a central determinant of reactor performance.

These imbalances can ultimately be translated into process deviations. Excessive accumulation may increase concentration polarization and reduce effective electrode utilization, whereas insufficient retention may reduce biological reaction capacity and electron-transfer capability. Both conditions may contribute to voltage fluctuations, changes in current density, lower substrate-conversion efficiency, and longer recovery after load changes. The model developed by Day et al. (2022) similarly showed that flow patterns, substrate removal, and current generation are interdependent in MFCs. The conceptual relationships between hydrodynamic conditions, biomass imbalance, electrochemical consequences, and operational reliability are summarized in Figure 4. The illustrated electrochemical and maintenance effects are literature-supported implications and were not measured directly in the present experiments.

An additional operational consideration is the trade-off between wastewater-treatment function and energy recovery. MFC operation requires sufficient microbial activity to degrade organic

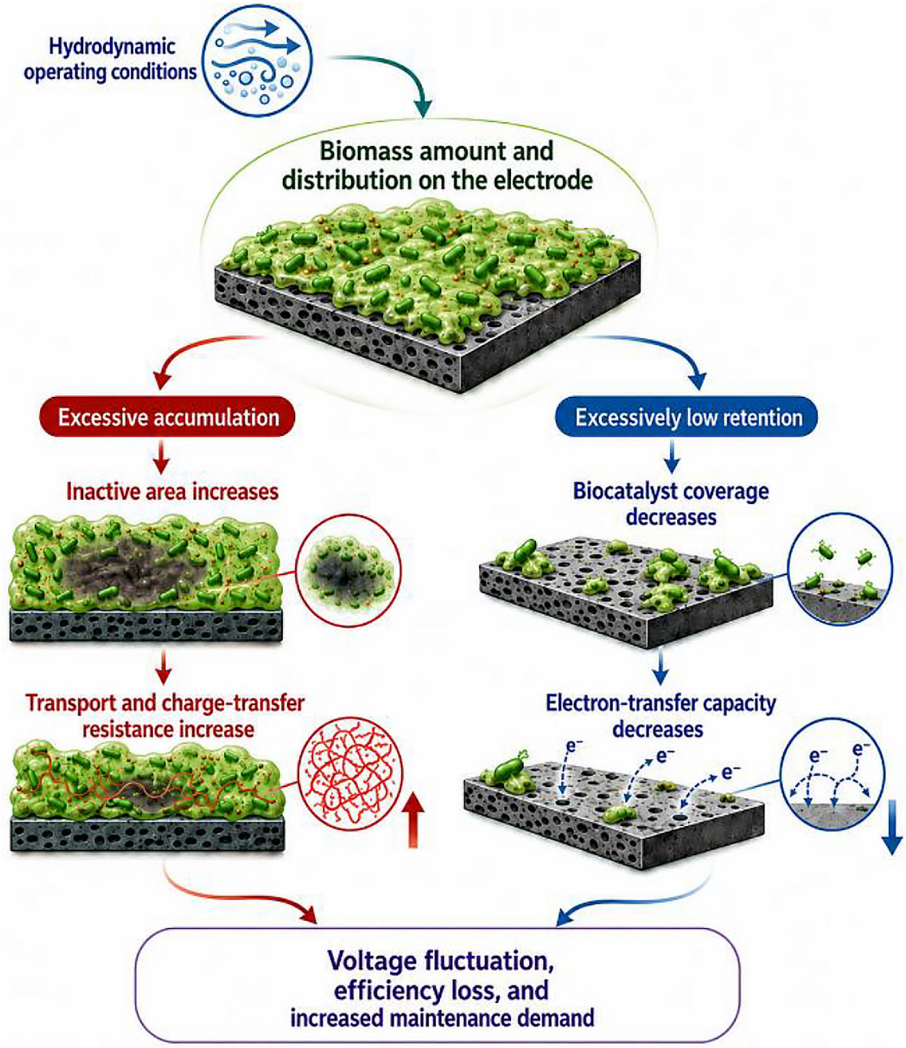

Figure 4. Conceptual pathway linking hydrodynamic operating conditions, biomass imbalance, electrochemical consequences, and operational reliability in bioelectrochemical systems

matter while ensuring that the resulting electrons are efficiently transferred to the electrode. A large biomass inventory may support substrate degradation but does not necessarily produce high Coulombic efficiency or power output if electrons are diverted to cell growth, side products, or pathways not connected to the electrode. Conversely, excessive biomass removal may reduce treatment capacity. Because the present system used a mixture of food-waste hydrolysate, Sidoarjo mud, and Shewanella oneidensis MR-1, its actual operational response may also depend on microbial-community interactions and substrate complexity.

The importance of this balance increases during scale-up. Larger bioelectrochemical reactors may develop nonuniform flow and substrate distributions, causing different areas of the same reactor to experience different levels of biomass accumulation. Consequently, an agitation speed that produces a particular response in a 1-L laboratory reactor cannot be transferred directly to a larger configuration without reassessing reactor geometry, flow distribution, electrode area, and organic loading (Fathima et al., 2024).

Biofilm-related operational problems are not limited to the anode. In membrane-less MFCs, unwanted microbial colonization of the cathode can cover active sites, restrict oxygen access, and impair the oxygen-reduction reaction. Barakat et al. (2025) associated severe cathode biofouling with decreases in cell potential, current density, and power during long-term operation. Nevertheless, the microbial-count data obtained in the present study cannot be used to claim cathode biofouling, pore blockage, or increased internal resistance because the location of biomass and the electrochemical consequences were not measured directly.

From a maintenance perspective, uncontrolled accumulation may increase the need for electrode inspection and cleaning, whereas frequent biomass detachment may cause solids release and instability of the microbial community. Overly aggressive cleaning may also remove the electroactive biofilm required for operation and extend the recovery period. Operational and maintenance strategies should therefore target selective control of inactive or excessive biomass rather than complete biofilm removal.

Bulk-suspension microbial count can consequently serve as one indicator of biological condition, but it is insufficient as the sole basis for operational decisions. A more complete monitoring strategy should combine suspended and electrode-associated biomass, viability, electrochemical response, substrate removal, hydrodynamic variables, energy demand, and maintenance indicators.

Hydrodynamic operating control as an inherently safer design-aligned strategy

Hydrodynamic operating control in bioelectrochemical systems should not be interpreted as maximizing agitation speed or maximizing total biomass. In the present study, the defensible objective is to avoid hydrodynamic extremes while recognizing that the available data do not identify a unique optimum or validated safe rpm. Agitation speed is therefore treated as a candidate preventive operating variable whose acceptable range must ultimately be verified using multiple biological, electrochemical, process, energy, and reliability indicators.

This approach is consistent with the philosophy of inherently safer design (ISD), which prioritizes elimination or reduction of hazards through changes in materials, technology, inventory, and operating conditions rather than relying exclusively on additional protective systems. The four commonly cited ISD principles are minimize, substitute, moderate, and simplify. The most relevant principle in the present context is moderation: operating conditions should be kept away from extremes so that the likelihood and consequences of deviations are reduced at their source (Amyotte and Khan, 2021; Hendershot, 2012).

The term inherently safer must nevertheless be used carefully. ISD is relative to a particular hazard or deviation, and an operating change that reduces one risk may increase another. A static condition may enhance biomass retention but promote nonuniform transport, whereas increased agitation may improve circulation while reducing biofilm retention. No single agitation condition can therefore be assumed to be inherently safer with respect to every possible failure mode.

The descriptive time courses motivate evaluation of an operating range rather than selection of a single optimum, but they do not resolve individual agitation speeds or establish an operating limit. Any rpm grouping in the present framework is a hypothesis-generating working classification. In biological systems, an acceptable hydrodynamic condition may also change with biofilm age, substrate concentration, fluid properties, microbial-community activity, electrode condition, and operating phase.

From an ISD perspective, moderation means avoiding conditions that create excessive dependence on corrective action. Inadequate mixing may eventually require manual intervention or cleaning after excessive accumulation develops, whereas excessive agitation may require a recovery period or reinoculation after substantial biomass loss. A more preventive strategy is to establish hydrodynamic conditions that limit the tendency toward either extreme during normal operation.

Agitation control through a motor, instrumentation, and control logic is an active safeguard and is therefore not inherently safer in the strictest sense. The more precise description is an operational strategy aligned with ISD, particularly with the principles of moderation and simplification. Such a strategy does not replace active controls, alarms, operating procedures, inspection, or maintenance; rather, it reduces the burden placed on those layers of protection (Center for Chemical Process Safety, 2019).

Implementation requires coordinated decisions at the design, operating, and monitoring levels. Reactor geometry, electrode placement, impeller configuration, and flow distribution should be selected to avoid stagnant or excessively stressed zones. During operation, agitation should be maintained around a defined target and bounded by warning and action limits. Biological, electrochemical, process, and equipment indicators should then be monitored to verify that the selected hydrodynamic condition continues to provide the intended function. This integrated implementation pathway is summarized in Figure 5. The framework integrates the hydrodynamic design basis, agitation targets and operating limits, controlled operation, and monitoring of biological, electrochemical, and

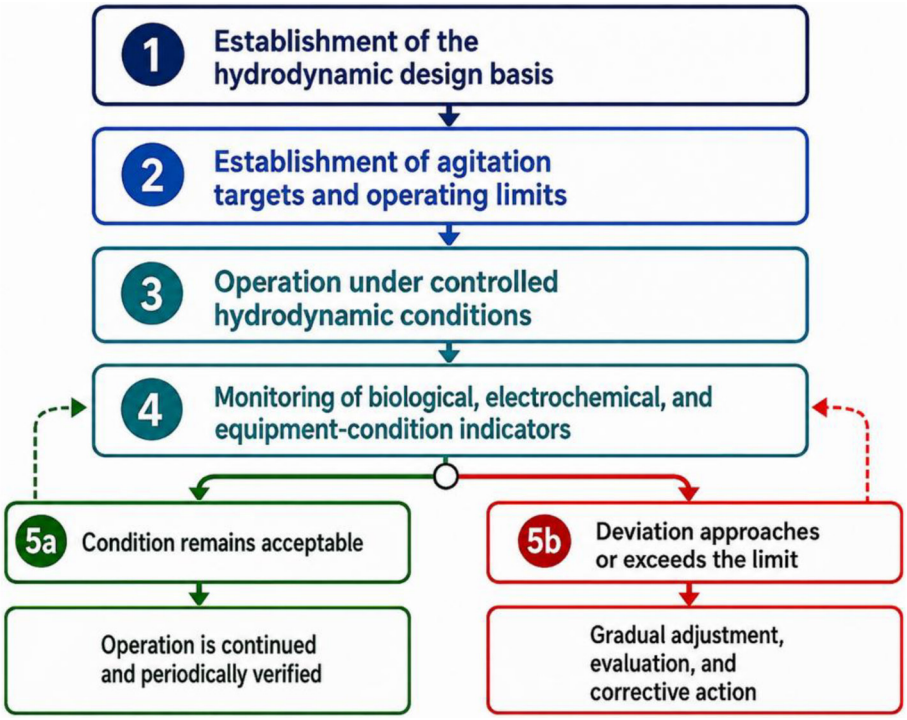

Figure 5. Conceptual framework for implementing hydrodynamic operating control as a preventive operational strategy aligned with inherently safer design principles

equipment indicators. Acceptable conditions support continued operation and periodic verification, whereas deviations approaching or exceeding the operating limits require gradual adjustment, evaluation, and corrective action.

As summarized in Figure 5, hydrodynamic operating control should be implemented as a continuous operational cycle rather than as a one-time selection of agitation speed. Monitoring results determine whether the system remains within an acceptable condition or requires gradual adjustment, further evaluation, and corrective action.

ISD principles should also be integrated into process safety management rather than treated as a stand-alone assessment. Hydrodynamic operating limits should be considered during hazard analysis, management of change, equipment-integrity programs, operating-procedure development, training, and incident investigation. Explicit integration of ISD into these management elements is more effective than using inherent safety only as a general design-stage concept (Amyotte et al., 2007; Rayner Brown et al., 2021).

Changes in agitation speed should be managed as changes in operating conditions. Before a set point is modified, the potential effects on mixing-energy demand, electrode condition, biological stability, biocatalytic function, and maintenance requirements should be considered. For an operating reactor, the transition period is also important because the biofilm response may lag behind the change in agitation.

Start-up and steady-state operation may require different hydrodynamic strategies. During start-up, microorganisms are still establishing initial colonization; an agitation speed tolerated by a mature biofilm may therefore be unsuitable during early attachment. Gradual ramping is preferable to an abrupt transition to the final set point because it moderates the rate of change and reduces the likelihood of forcing the developing biofilm outside an acceptable operating condition.

Operational decisions should be based on multiple success criteria. Bulk-suspension total cell count is the only quantitative biological response available across agitation conditions in the present archive, and a safer or more reliable condition cannot be identified by maximizing or minimizing this variable alone. Future implementation should consider the combined stability of suspended and attached biomass, cell viability, voltage, current density, internal resistance, Coulombic efficiency, organic-matter removal, mixing-energy demand, and maintenance frequency.

It is also important to distinguish among a normal set point, a warning limit, and an action limit.

The normal set point represents the target for stable operation. A warning limit indicates that the system is moving away from the desired condition but can still be corrected without interruption. An action limit indicates a sufficiently large deviation to justify operating adjustment, inspection, or temporary shutdown. The present dataset is insufficient to define these limits numerically, but it provides an initial basis for developing such a structure.

Scale-up further limits the direct use of rpm as a universal parameter. Agitation speed is specific to reactor dimensions, impeller type, electrode geometry, fluid properties, and working volume. More transferable hydrodynamic parameters include power input per unit volume, superficial velocity, mixing time, Reynolds number, shear rate, and estimated shear stress. Laboratory trends can indicate the direction of the agitation effect, but operating limits must be re-established for each reactor configuration (Corona-Martínez et al., 2025; Fathima et al., 2024).

Simplification is equally important. An operating strategy with numerous set points and complex rules may increase the likelihood of operator error. Hydrodynamic guidance should therefore be documented in a clear and monitorable form, with predefined criteria for when agitation should be increased, decreased, or maintained. Deviations should trigger consistent actions such as electrode inspection, evaluation of the electrochemical response, and assessment of cleaning requirements.

Hydrodynamic control should not be presented as a substitute for other risk-management measures. Changes in substrate composition, contamination, electrical disturbances, electrode damage, and microbial-community instability may still occur. Hydrodynamic operating control should therefore form part of a layered strategy that includes appropriate equipment design, monitoring, procedures, inspection, and maintenance.

Overall, agitation can be positioned as a candidate strategic variable for avoiding hydrodynamic extremes. In this study, the concept represents a structured compromise and monitoring framework rather than a mathematically determined optimum, a validated rpm value, or a quantified safety margin. This evidence-limited preventive concept is formalized in the following section as a preliminary conceptual Safe Hydrodynamic Operating Window (SHOW).

Proposed preliminary conceptual safe hydrodynamic operating window (SHOW)

Based on the descriptive time courses and the preceding mechanistic and operational interpretation, this study proposes SHOW as a preliminary conceptual framework for translating hydrodynamic observations into structured operating guidance. SHOW is not intended to identify a universally applicable agitation speed or certify a numerical safety margin. Instead, it defines how an acceptable hydrodynamic region could be established in future work by jointly considering bulk and attached biomass, bioelectrochemical function, process performance, energy demand, and operational reliability.

An operating window represents a range of parameters that produces an acceptable process response. This differs from a single optimum because several operating conditions may provide comparably acceptable performance. Conceptually, SHOW is analogous to a design space: the acceptable region is established from the combined relationships between operating parameters and relevant process responses and should be revised when process knowledge, scale, or equipment changes (International Council for Harmonisation, 2009).

In the present study, nominal agitation speed was the controlled hydrodynamic variable and bulk-suspension total cell concentration was the measured biological response. The descriptive means across days 0–20 were 6.644×10^6, 3.044×10^6, 2.594×10^6, 2.254×10^6, 1.028×10^6, and 3.32×10^5 cells mL^{-1} at 0, 50, 100, 150, 200, and 250 rpm, respectively. Because independent reactor replication is not documented, no numerical SHOW boundary can be statistically validated from this dataset.

The framework is divided into three literature-informed, hypothesis-generating regions: Region I, a low-mixing reference; Region II, a candidate study region; and Region III, a higher-agitation reference. These regions organize future testing and must not be interpreted as measured biofilm states, proven safety boundaries, or causal classifications.

Region I – Low-mixing hypothesis. The 0-rpm condition is retained as the low-mixing reference because it had the highest descriptive mean bulk-suspension count. However, a high suspended-cell count does not demonstrate attached-biomass accumulation or the most stable electrochemical operation. A defensible lower hydrodynamic boundary would require direct

Table 2. Evaluation dimensions, acceptance concept, and evidence status for future SHOW validation

Evaluation dimension	Future SHOW acceptance concept	Evidence in the present archive
Biological	Suspended and attached viable biomass remain sufficient and stable.	Bulk total-cell count measured; electrode biomass, viability, EPS, and biofilm thickness not measured.
Electrochemical	Voltage, current, power density, and resistance remain acceptable.	Not measured across agitation conditions.
Treatment performance	Substrate/COD removal meets the required target.	Not measured across agitation conditions.
Hydrodynamic	Mixing is sufficiently uniform without excessive local stress.	Nominal rpm recorded; agitator geometry, shear stress/rate, and mixing uniformity not retained.
Operational	Cleaning and recovery demands remain acceptable.	Long-term recovery, cleaning demand, and reliability not measured.
Energy	Mixing-energy demand does not exceed the performance benefit.	Mixing-energy demand not measured.

evidence of mixing adequacy, attached biomass, mass transfer, treatment performance, and electrochemical function.

Region II – Descriptive candidate study region. The 50–150 rpm conditions had descriptive mean bulk-suspension counts between 2.254 × 10^6 and 3.044 × 10^6 cells mL^{-1}. This interval is retained only to focus future independently replicated experiments at narrower hydrodynamic intervals. It is not claimed to be safe, optimal, statistically superior, or representative of verified biofilm retention. Only bulk-suspension total cell concentration was measured as a response to agitation in the present archive, and even this dimension does not establish viability, electrode-associated biomass, biofilm quality, or electroactive function. The electrochemical, treatment-performance, hydrodynamic-stress, operational-reliability, and energy dimensions in Table 2 are therefore explicit future validation requirements rather than measured evidence.

Region III – Higher-agitation hypothesis. The 200- and 250-rpm conditions had descriptive mean bulk-suspension counts of 1.028 × 10^6 and 3.32 × 10^5 cells mL^{-1}, respectively; the 250-rpm mean was approximately 5.0% of the 0-rpm mean. These lower bulk counts do not demonstrate that an electrode-biomass, process-failure, or safety threshold was crossed. Such a classification requires concurrent unacceptable changes in attached biomass, viability, electrochemical performance, treatment, recovery, or reliability indicators.

Accordingly, an upper SHOW boundary cannot be assigned from this dataset. A validated upper

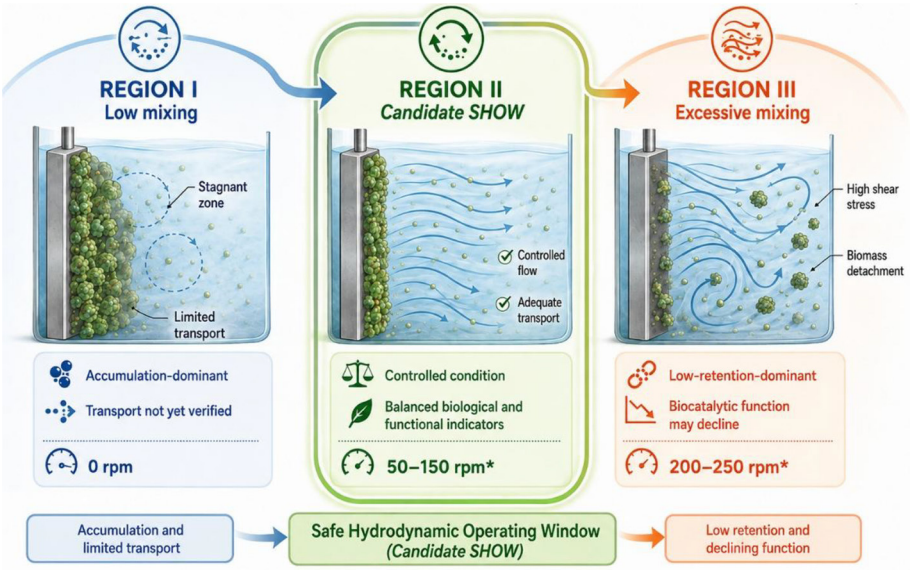

Figure 6. Preliminary conceptual SHOW framework. The indicated rpm groupings are descriptive candidate regions and do not constitute statistically validated safety boundaries

boundary would require independently replicated evidence that increased hydrodynamic intensity produces a sustained unacceptable biological, electrochemical, treatment, energy, or maintenance response. The three-region diagram in Figure 6 is therefore a conceptual map for future validation, not a validated numerical operating envelope.

Region II should not be interpreted as safe in an absolute or validated sense. Here, "safe" denotes the intended future function of an operating window assessed and bounded using multiple relevant indicators; it does not mean that 50–150 rpm has been validated as safe or that all risks are eliminated. This interpretation is consistent with inherently safer design, which emphasizes relative risk reduction and moderation of operating extremes.

SHOW should ultimately incorporate four categories of boundaries. The biological boundary is reached when microbial count or viability moves outside the range required for biocatalytic function. The electrochemical boundary is reached when voltage, current, power density, or internal resistance shows an unacceptable deviation. The process boundary is reached when substrate removal, pH, conductivity, or another treatment variable no longer meets its target. The operational boundary is reached when mixing-energy demand, cleaning, recovery, or maintenance requirements increase disproportionately. The validated SHOW would be the intersection of all acceptable ranges rather than the range of a single response variable.

In its present form, SHOW is a single-response, hypothesis-generating framework informed by bulk-suspension microbial-count trends and literature mechanisms. Validation requires independently replicated reactors and narrower hydrodynamic intervals together with suspended and attached biomass, microbial viability, biofilm thickness and EPS, shear stress or shear rate, voltage, current/power density, internal resistance, Coulombic efficiency, COD/substrate removal, mixing-energy consumption, and long-term operational-reliability measurements.

Agitation speed should also not be the sole basis for transferring SHOW to another reactor or a larger scale. Hydrodynamic operating windows should be evaluated in terms of more representative variables such as shear rate, shear stress, power input per unit volume, superficial velocity, mixing time, and relevant dimensionless numbers. Scale-up must account for nonuniform flow distribution, changes in internal resistance, electrode arrangement, and substrate distribution (Corona-Martínez et al., 2025; Fathima et al., 2024).

Finally, SHOW should be treated as a living framework that evolves with process knowledge. Initial candidate regions can be informed by laboratory observations, but validated boundaries should be refined using multivariable experimental evidence, operating trends, disturbances, maintenance history, and responses to substrate variability. The contribution of the present study is therefore a structured method for defining what should be measured, monitored, and updated when establishing hydrodynamic operating limits, rather than the assertion of a final safe rpm range.

Study limitations and evidence boundaries

The evidence base has several limitations. First, the archive contains five longitudinal sampling days per agitation condition but no documented independent reactor replication, so treatment-level inferential testing is not justified. Second, only direct total-cell counts from the bulk reactor matrix were preserved; electrode-associated biomass, viability, and the electroactive fraction were not measured. Third, the underlying five chamber-area readings for each reported observation and several counting-chamber details were not retained. Fourth, local shear stress, hydrodynamic hardware details, biofilm characteristics, electrochemical performance, substrate removal, mixing-energy demand, and long-term reliability were not measured. Finally, rpm is equipment-specific and cannot be transferred directly across reactor geometries or scales. These limitations prevent validation of a numerical safety margin or universal hydrodynamic operating window.

The original 30 reported observations, a data dictionary, descriptive summaries, and the surviving microbial-enumeration protocol are supplied in Supplementary Data S1. The supplement explicitly identifies the measured fraction as bulk reactor suspension and lists unretained metadata without substituting fabricated values. The present SHOW must therefore be interpreted strictly as a preliminary conceptual framework supported by a descriptive time course.

CONCLUSIONS

The surviving archive shows a strong descriptive agitation-related gradient in bulk-suspension

microbial counts. The mean across days 0–20 decreased from 6.644×10^6 cells mL^{-1} at 0 rpm to 3.32×10^5 cells mL^{-1} at 250 rpm, a 95.0% difference, while the 200 and 250-rpm series peaked on day 10 and subsequently declined. Because the five values per condition are repeated time points without documented independent reactor replication, the data do not support independent-groups inferential testing, a causal biofilm-detachment claim, or a statistically validated rpm threshold. The 50–150 rpm interval is retained only as a candidate region for future independently replicated validation. SHOW remains a preliminary conceptual framework requiring direct measurements of attached biofilm, viability, hydrodynamic stress, electrochemical performance, treatment performance, energy demand, and long-term operational reliability.

REFERENCES

1. Aelterman, P., Rabaey, K., Pham, H. T., Boon, N., Verstraete, W. (2006). Continuous electricity generation at high voltages and currents using stacked microbial fuel cells. *Environmental Science & Technology*, *40*(10), 3388–3394. https://doi.org/10.1021/es0525511
2. Akbar, R. A., Anityasari, M., Arriyanto, R. J., Melchior, I. D., Septaprasetya, A. C., Santoso, T. B. (2025). Occupational health and safety risk assessment of Surabaya pump houses using the HIRARC (Hazard Identification, Risk Assessment, and Risk Control) method. *JMES: The International Journal of Mechanical Engineering and Sciences*, *9*(2), 80–88. https://doi.org/10.12962/j25807471.v9i2.22624
3. Amyotte, P. R., Goraya, A. U., Hendershot, D. C., Khan, F. I. (2007). Incorporation of inherent safety principles in process safety management. *Process Safety Progress*, *26*(4), 333–346. https://doi.org/10.1002/prs.10217
4. Amyotte, P. R., Khan, F. I. (2021). The role of inherently safer design in process safety. *The Canadian Journal of Chemical Engineering*, *99*(4), 853–871. https://doi.org/10.1002/cjce.23987
5. Aopik, A., Dwiyantoro, B. A. (2023). Numerical study of reducer modification with adjuster opening variations on turbine lube oil pipe. *JMES: The International Journal of Mechanical Engineering and Sciences*, *7*(1), 17–25. https://doi.org/10.12962/j25807471.v7i1.12065
6. Barakat, N. A. M., Gamal, H., Osama, R. (2025). Mitigating cathode biofouling in membrane-less MFCs using CuO-doped activated carbon: A comparative study of batch and continuous modes. *Scientific Reports*, *15*, Article 41465. https://doi.org/10.1038/s41598-025-27118-2
7. Bond, D. R., Lovley, D. R. (2003). Electricity production by *Geobacter sulfurreducens* attached to electrodes. *Applied and Environmental Microbiology*, *69*(3), 1548–1555. https://doi.org/10.1128/AEM.69.3.1548-1555.2003
8. Center for Chemical Process Safety. (2019). *Guidelines for inherently safer chemical processes: A life cycle approach* (3rd ed.). John Wiley & Sons.
9. Chen, H., Xia, A., Yan, H., Huang, Y., Zhu, X., Zhu, X., Liao, Q. (2024). Mass transfer in heterogeneous biofilms: Key issues in biofilm reactors and AI-driven performance prediction. *Environmental Science and Ecotechnology*, *22*, Article 100480. https://doi.org/10.1016/j.ese.2024.100480
10. Corona-Martínez, D. A., Martínez-Amador, S. Y., Rodríguez-De la Garza, J. A., Laredo-Alcalá, E. I., Pérez-Rodríguez, P. (2025). Recent advances in scaling up bioelectrochemical systems: A review. *BioTech*, *14*(1), Article 8. https://doi.org/10.3390/biotech14010008
11. Day, J. R., Heidrich, E. S., Wood, T. S. (2022). A scalable model of fluid flow, substrate removal and current production in microbial fuel cells. *Chemosphere*, *291*, Article 132686. https://doi.org/10.1016/j.chemosphere.2021.132686
12. Fathima, A., Ilankoon, I. M. S. K., Zhang, Y., Chong, M. N. (2024). Scaling up of dual-chamber microbial electrochemical systems—An appraisal using a systems design approach. *Science of the Total Environment*, *912*, Article 169186. https://doi.org/10.1016/j.scitotenv.2023.169186
13. Flemming, H.-C., van Hullebusch, E. D., Neu, T. R., Nielsen, P. H., Seviour, T., Stoodley, P., Wingender, J., Wuertz, S. (2023). The biofilm matrix: Multitasking in a shared space. *Nature Reviews Microbiology*, *21*(2), 70–86. https://doi.org/10.1038/s41579-022-00791-0
14. Flemming, H.-C., Wingender, J., Szewzyk, U., Steinberg, P., Rice, S. A., Kjelleberg, S. (2016). Biofilms: An emergent form of bacterial life. *Nature Reviews Microbiology*, *14*(9), 563–575. https://doi.org/10.1038/nrmicro.2016.94
15. Godain, A., Vogel, T. M., Fongarland, P., Haddour, N. (2024). Influence of shear stress on electroactive biofilm characteristics and performance in microbial fuel cells. *Biosensors and Bioelectronics*, *244*, Article 115806. https://doi.org/10.1016/j.bios.2023.115806
16. Hendershot, D. C. (2012). Inherently safer design: The fundamentals. *Chemical Engineering Progress*, *108*(1), 40–42.
17. International Council for Harmonisation. (2009). *ICH harmonised tripartite guideline Q8(R2): Pharmaceutical development*. https://database.ich.org/sites/default/files/Q8_R2_Guideline.pdf
18. Islam, M. A., Ehiraj, B., Cheng, C. K., Dubey, B. N., Khan, M. M. R. (2019). Biofilm re-vitalization

using hydrodynamic shear stress for stable power generation in microbial fuel cells. *Journal of Electroanalytical Chemistry*, *844*, 14–22. https://doi.org/10.1016/j.jelechem.2019.05.013

19. Laily, F. N., Juliastuti, S. R., Darmawan, R., Dusabe, S., Hendrianie, N., Rachmaniah, O., Nurhikmah, N., Putraditama, N. R. (2023). Production of electricity from food waste using microbial fuel cell and hydrolytic microorganisms. AIP Conference Proceedings, 2667, 030008. https://doi.org/10.1063/5.0112304
20. Liu, Y., Tay, J.-H. (2002). The essential role of hydrodynamic shear force in the formation of biofilm and granular sludge. *Water Research*, *36*(7), 1653–1665. https://doi.org/10.1016/S0043-1354(01)00379-7
21. Logan, B. E., Hamelers, B., Rozendal, R., Schröder, U., Keller, J., Freguia, S., Aelterman, P., Verstraete, W., Rabaey, K. (2006). Microbial fuel cells: Methodology and technology. *Environmental Science & Technology*, *40*(17), 5181–5192. https://doi.org/10.1021/es0605016
22. Logan, B. E., Rossi, R., Ragab, A. A., Saikaly, P. E. (2019). Electroactive microorganisms in bioelectrochemical systems. *Nature Reviews Microbiology*, *17*(5), 307–319. https://doi.org/10.1038/s41579-019-0173-x
23. Marcus, A. K., Torres, C. I., Rittmann, B. E. (2007). Conduction-based modeling of the biofilm anode of a microbial fuel cell. *Biotechnology and Bioengineering*, *98*(6), 1171–1182. https://doi.org/10.1002/bit.21533
24. Nugroho, A., Ariyanto, E. D., Ariyanto, S. R., Arifianti, L. S. Y., Hsiau, S.-S. (2026). Enhancing biocrude and hydrochar production from water hyacinth via hydrothermal processing and particle flow analysis. *JMES: The International Journal of Mechanical Engineering and Sciences*, *10*(1), 45–54. https://doi.org/10.12962/j25807471.v10i1.23489
25. Pant, D., Van Bogaert, G., Diels, L., Vanbroekhoven, K. (2010). A review of the substrates used in microbial fuel cells (MFCs) for sustainable energy production. *Bioresource Technology*, *101*(6), 1533–1543. https://doi.org/10.1016/j.biortech.2009.10.017
26. Petrova, O. E., Sauer, K. (2012). Sticky situations: Key components that control bacterial surface attachment. *Journal of Bacteriology*, *194*(10), 2413–2425. https://doi.org/10.1128/JB.00003-12
27. Picioreanu, C., Head, I. M., Katuri, K. P., van Loosdrecht, M. C. M., Scott, K. (2007). A computational model for biofilm-based microbial fuel cells. *Water Research*, *41*(13), 2921–2940. https://doi.org/10.1016/j.watres.2007.04.009
28. Rayner Brown, K., Hastie, M., Khan, F. I., Amyotte, P. R. (2021). Inherently safer design protocol for process hazard analysis. *Process Safety and Environmental Protection*, *149*, 199–211. https://doi.org/10.1016/j.psep.2020.10.046
29. Reguera, G., Nevin, K. P., Nicoll, J. S., Covalla, S. F., Woodard, T. L., Lovley, D. R. (2006). Biofilm and nanowire production leads to increased current in *Geobacter sulfurreducens* fuel cells. *Applied and Environmental Microbiology*, *72*(11), 7345–7348. https://doi.org/10.1128/AEM.01444-06
30. Santoro, C., Arbizzani, C., Erable, B., Ieropoulos, I. (2017). Microbial fuel cells: From fundamentals to applications. A review. *Journal of Power Sources*, *356*, 225–244. https://doi.org/10.1016/j.jpowsour.2017.03.109
31. Sasongko, H., Rahman, W. A. (2023). Numerical study of damper plate and nozzle effect on vortex turbine basin for increasing flow kinetic energy entering turbine rotor. *JMES: The International Journal of Mechanical Engineering and Sciences*, *7*(1), 54–63. https://doi.org/10.12962/j25807471.v7i1.16270
32. Slate, A. J., Whitehead, K. A., Brownson, D. A. C., Banks, C. E. (2019). Microbial fuel cells: An overview of current technology. *Renewable and Sustainable Energy Reviews*, *101*, 60–81. https://doi.org/10.1016/j.rser.2018.09.044
33. Stoodley, P., Lewandowski, Z., Boyle, J. D., Lappin-Scott, H. M. (1999). Structural deformation of bacterial biofilms caused by short-term fluctuations in fluid shear: An in situ investigation of biofilm rheology. *Biotechnology and Bioengineering*, *65*(1), 83–92. https://doi.org/10.1002/(SICI)1097-0290(19991005)65:1%3C83::AID-BIT10%3E3.0.CO;2-B
34. Wulaningtyas, O., Yuwono, T. Y. (2025). Numerical study of the installation configuration of four Savonius hydrokinetic turbines in the cooling water channel of PAITON Power Plant. *JMES: The International Journal of Mechanical Engineering and Sciences*, *9*(1), 24–31. https://doi.org/10.12962/j25807471.v9i1.21937
35. Yang, P., Gao, Y., Wang, N., Zhu, Y., Xue, L., Han, Y., Liu, J., He, W., Feng, Y. (2023). The restricted mass transfer inside the anode pore channel affects electroactive biofilm formation, community composition, and power production in microbial electrochemical systems. *Science of the Total Environment*, *898*, Article 165448. https://doi.org/10.1016/j.scitotenv.2023.165448